

## Article

# Trace Elements in Sediments of Two Lakes in the Valley of the Middle Courses of the Ob River (Western Siberia)

Vladimir P. Shevchenko <sup>1,\*</sup>, Dina P. Starodymova <sup>1</sup>, Sergey N. Vorobyev <sup>2</sup>, Ramiz A. Aliev <sup>3</sup>,  
Lyudmila P. Borilo <sup>2</sup>, Larisa G. Kolesnichenko <sup>2</sup>, Artyom G. Lim <sup>2</sup>, Andrey I. Osipov <sup>1</sup>, Vladislav V. Trufanov <sup>4</sup>  
and Oleg S. Pokrovsky <sup>2,5</sup>

<sup>1</sup> Shirshov Institute of Oceanology, Russian Academy of Sciences, Nakhimovsky Prospect, 36, 117997 Moscow, Russia

<sup>2</sup> BIO-GEO-CLIM Laboratory, Tomsk State University, 36, Lenin Avenue, 634050 Tomsk, Russia

<sup>3</sup> Chemistry Department, Lomonosov Moscow State University, Leninskie Gory, 119991 Moscow, Russia

<sup>4</sup> Geological Department, Lomonosov Moscow State University, Leninskie Gory, 119234 Moscow, Russia

<sup>5</sup> Geosciences and Environment Toulouse, UMR 5563 CNRS, University of Toulouse, 14 Avenue Edouard Belin, 31400 Toulouse, France

\* Correspondence: vshevch@ocean.ru

**Abstract:** Lake sediments accumulate various pollutants and act as efficient natural archives suitable for reconstruction the environmental conditions of the past. In contrast to fairly good knowledge of mineral sediments in lakes of European and North America boreal lakes, Siberian lakes of the boreal zone remain quite poorly studied. In this work, two cores of lake sediments of the Ob River valley were investigated. Elemental analyses were carried out on the sediments, losses on ignition were determined, and the rate of sedimentation was measured from the activity of Pb-210 and Cs-137. According to the content of organic matter, bottom sediments belong to different types: clastic (Lake Inkino, located in the Ob River floodplain) and organogenic (Lake Shchuchie on the second terrace). The rate of sedimentation in Lake Shchuchie is several times higher than that in Lake Inkino. The sediments of Lake Inkino are similar in composition (including the pattern of rare earth elements) to the suspended particulate matter of the Ob River as well as to average detrital matter of the upper continental crust. Sediments of Lake Shchuchie (sapropels) are enriched in a number of heavy metals. Based on the elemental composition, signs of diagenetic processes and authigenic mineral formation were determined, such as accumulation of carbonates and the formation of manganese oxides and hydroxides. There is an enhanced recent input of Cr, Co, Cu, Zn, Cd, Sb, Pb, and Bi in the upper layers of sediments as a result of atmospheric anthropogenic pollutant deposition.

**Keywords:** lake bottom sediments; western Siberia; Ob River valley; floodplain; sapropel; rate of sedimentation; elemental composition; REE; pollution



**Citation:** Shevchenko, V.P.; Starodymova, D.P.; Vorobyev, S.N.; Aliev, R.A.; Borilo, L.P.; Kolesnichenko, L.G.; Lim, A.G.; Osipov, A.I.; Trufanov, V.V.; Pokrovsky, O.S. Trace Elements in Sediments of Two Lakes in the Valley of the Middle Courses of the Ob River (Western Siberia). *Minerals* **2022**, *12*, 1497. <https://doi.org/10.3390/min12121497>

Academic Editor: Pierfranco Lattanzi

Received: 11 October 2022

Accepted: 21 November 2022

Published: 24 November 2022

**Publisher's Note:** MDPI stays neutral with regard to jurisdictional claims in published maps and institutional affiliations.



**Copyright:** © 2022 by the authors. Licensee MDPI, Basel, Switzerland. This article is an open access article distributed under the terms and conditions of the Creative Commons Attribution (CC BY) license (<https://creativecommons.org/licenses/by/4.0/>).

## 1. Introduction

Lake sediments tend to accumulate various pollutants; therefore, they are efficient natural archives and can be used to reconstruct the environmental conditions of the past [1–9]. A unique feature of lake sediments is that their rate of accumulation is tens to hundreds of times higher than that in adjacent seas, and thus, the resolution of stratigraphic methods is much higher in lakes than in the seas [2,10].

Undisturbed bottom sediments contain records of past environments and allow for the establishment of background levels of input of some pollutants [2–5,11]. Lake sediments composition reflects the conditions and processes that occurred in lake and its watershed throughout the history of sediment formation. Particles originating in watershed are deposited in lakes. Therefore, lake sediments can be used to display spatial variation of trace elements in different regions, and thus, lake sediments may serve as a medium in evaluating the background concentration of metals [1,12]. Early diagenesis processes

occurring in lake sediments are responsible for post-deposition mineralization of organic matter and therefore play an important role in sediment matter transformation and controls the post-depositional redistribution of trace elements [13].

Atmospheric transport is an important pathway for the entry of dispersed sedimentary matter and trace element contamination into oceans, seas, and lakes [14–16]. Lacustrine sediments of some industrialized regions are well-studied in relation to the accumulation of heavy metals (Cu, Ni, Zn, Pb, etc.) [2,3,17,18]. Sediments of lakes remote from local sources of anthropogenic pollution accumulate information on the influx of pollutants from the atmosphere, essentially from global sources, via long-range atmospheric transfer. This makes it possible to trace changes in atmospheric pollution and compare the current level with the pre-industrial period [1,19–23].

There are several works of the accumulation of heavy metals by lake sediments performed in the south and north of western Siberia [11,23–27]. However, the lakes in the southern taiga zone of western Siberia have been studied to a lesser extent. There are small lakes in the Ob River middle course flooded during spring period, located within large rivers floodplains, and upland lakes situated at the upper terraces of the river that are not flooded during the spring period [28]. Upland lakes serve as a major source of dissolved organic carbon, metals, and other solutes to the rivers and small streams and are subjected to strong influence of mires [28].

The present study is aimed at filling the gap in knowledge of lake sediments of the western Siberian boreal zone, and it focuses on resolving spatial variation of trace element concentration in sediments and quantifying rate of sediment accumulation of two contrasting lakes of the region—a floodplain lake and a terrace lake, both located within the middle course of the Ob River in the boreal taiga zone.

## 2. Materials and Methods

### 2.1. Sampling Sites Description

Lake Inkino (Ink) is located in the floodplain (2.3 km from the main stem) of the middle course of Ob River on its left bank (Figure 1). The area of the lake is 77,100 m<sup>2</sup>, and the average depth is 3.5 m. The bottom of the lake is muddy with a great deal of decomposed organic matter. Vegetation along the coast is forb-canary grass-sedge meadows. Lake Shchuchie (Sch) is located on the 2nd upper terrace of the Ob River (right bank), 4.9 km from the main stem. The area of the lake is 160,600 m<sup>2</sup>, and the average depth is 7.8 m. The bottom is also muddy, but unlike the floodplain lake, Lake Shchuchie's sediments are dominated by well-decomposed peat. Vegetation along the lake shore is represented by birch-pine and pine-birch forest. The lake is surrounded by a transitional bogs (sphagnum-forb, woody shrub-sphagnum-grass, and pine sphagnum-sedge bog). The distance between two sampling sites is approximately 23 km.

### 2.2. Sample Collection and Description

Sampling was performed in Lakes Inkino and Shchuchie during the summer baseflow period in August 2020 using an inflatable boat. One sediment core was collected from each lake using a Large Bore Interface Corer (Aquatic Research Instruments®, Hope, ID, USA) equipped with a polycarbonate core tube (60 cm length, 10 cm inner diameter). The corer was manually inserted into non-perturbed sediment.

The core Ink, 36 cm long, is represented by a clayey-muddy sediment dark gray in color that is also homogeneous and slightly lightened in the upper part. Weak layering is identified. Small soft nodules of a light brown color, up to 1 mm in diameter, are rarely scattered in the lower part of the core. In the upper part of the core, there are semi-decomposed small pieces of herbaceous plants. At all depths, there is a smell of hydrogen sulfide. The sampled core was subdivided into 1 cm layers down to a depth of 14 cm and into 2 cm layers deeper.

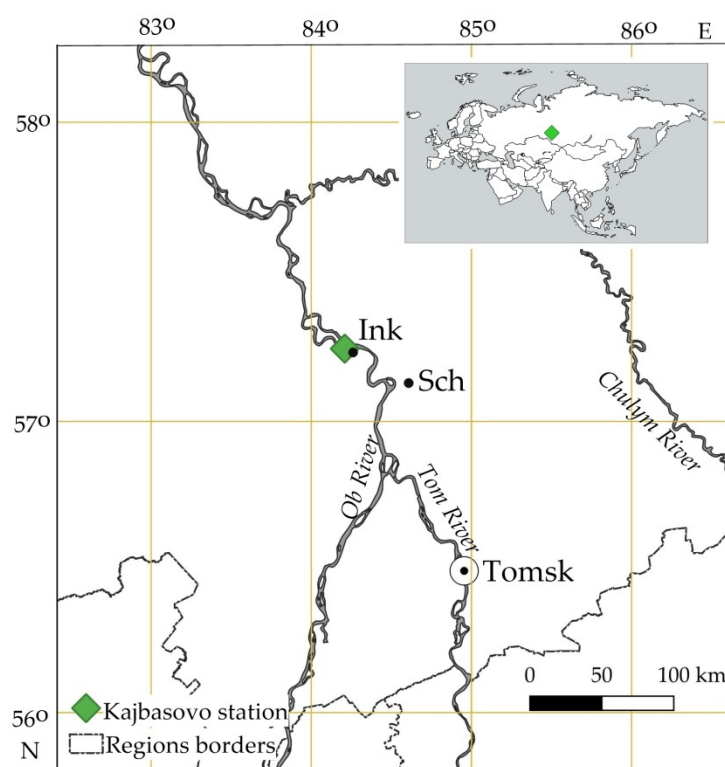


**Figure 1.** Map of sampling sites.

The core Sch, 24 cm long, is represented by dark brown muddy sediment that is homogeneous and darker to black in the lower part. Interlayering with layers of a darker color occurs in core. In the upper part, sediments are enriched with the remains of decomposed organic matter. There are inclusions of well-decomposed and semi-decomposed peat at all depths. Soft black concretions up to 2 mm in diameter are found in the lower part of the core. At all depths, there is a smell of hydrogen sulfide. The sampled core was subdivided into 1 cm layers down to a depth of 10 cm and into 2 cm layers deeper.

In the laboratory, the samples were dried in a freeze dryer Martin Christ Alpha 2–4 LDplus and ground to powder in planetary mill Fritsch Pulverisette.

### 2.3. Elemental Analysis and Determination of Loss on Ignition

Samples were digested with a mixture of concentrated acids ( $\text{HClO}_4$ , HF,  $\text{HNO}_3$ , HCl,  $\text{H}_3\text{BO}_3$ ) in open Teflon reactors. Aliquots of  $^{145}\text{Nd}$ ,  $^{161}\text{Dy}$ , and  $^{174}\text{Yb}$  were used to control the chemical output during the sample digestion procedure. An internal standard (In) was used to monitor instrument drift. The quality of the analytical procedure was controlled by processing a blank sample and the reference materials ST-2a CRM № 8671-2005 (trap powder) and BHVO-2 (basalt powder). The elemental composition of sediments was determined using atomic emission spectroscopy (ICP-AES) and inductively coupled plasma mass spectrometry (ICP-MS). For atomic emission determination, an iCAP-6500 spectrometer from Thermo Scientific (USA) was used. For ICP MS, an X-7 mass spectrometer from Thermo Elemental (USA) was used. These methods determined the concentrations of the following elements: Na, Mg, Al, P, S, K, Ca, Ti, Mn, Fe (ICP-OES) Li, Be, B, Sc, V, Cr, Mn, Co, Ni, Cu, Zn, Ga, As, Se, Rb, Sr, Y, Zr, Mo, Nb, Ag, Cd, In, Sn, Sb, Te, Cs, Ba, REE, Hf, Ta, W, Tl, Pb, Bi, Th, and U (ICP-MS). The detection limit (DL) of the elements was defined as

$$\text{DL} = C_i + 3s$$

where  $C_i$  is the average content of element  $i$  when measuring procedure blank samples;  $s$  is the standard deviation for element  $i$  when measuring procedure blank samples. DLs varies depending on the method and element. ICP-OES DLs varies from 0.00001 (Mn) to 0.013

(Ca) m/m%, and ICP-MS DLs were 0.03 (for Tl) to 0.9 µg/g (for Cu and Zn). Accuracy of the measurements varies depending on the element. In general, measured concentrations of CRM are within 9% of their expected values. Precision of the measurements for all elements determined by the ICP-OES method did not exceed 20% when measuring the content of these elements up to 5 DL and 10% when measuring the content of more than 5 DL. Precision of the measurements for all elements measured by ICP-MS did not exceed 30% when the content of these elements was measured up to 5\*DL and did not exceed 15% when the content was measured >5 DL. Further details of the analytical procedure are provided in ref. [29].

Loss on ignition (LOI) at 550 °C was determined in sub-samples for estimating organic content in sediments according to [30]. Note that at this temperature, no decomposition of carbonates occurs. Therefore, the LOI value can be considered as a fast, inexpensive method of approximating for determining organic matter contents in sediments with precision and accuracy comparable to other more sophisticated geochemical methods that are widely used in paleolimnology [30–32]. However, it should be noted that the value of LOI also includes chemically bound water. We did not use a dehydration step at 150 °C (see, e.g., [33,34]) to account for hydrated minerals (e.g., gypsum) because such minerals are either unlikely to form in acidic and organic-rich lake waters (Shchuchie) or have not been identified in the Ob River suspended matter [35], which dominates the sediment formation in Inkino.

#### 2.4. Radioactivity Measurements

Between 1 and 8 g of freeze-dried sediments were placed in a container of cylindrical geometry, and the gamma-ray spectrum was measured on an HPGe GEM-C5060P4-B detector (Ortec, Ametek Inc., Berwyn, PA, USA) for ~90,000 s. The radioactivity of <sup>210</sup>Pb was determined using the 46.5 keV gamma line <sup>137</sup>Cs from the 661.6 keV line. For efficiency calibration, standard materials IAEA 447 (moss-soil) and IAEA 448 (soil from oil field) were used. The spectra were processed using the SpectraLine software, (LRSM, Russia, version 1.4.2792). Radium-226 activity, determined via the <sup>214</sup>Bi 609 keV gamma line, was below the detection limit in all samples (<30 Bq/kg). Therefore, all <sup>210</sup>Pb signals were considered as nonequilibrium.

Quantification of sedimentation rates was carried out according to the model of constant initial concentration [36–38], in which it is assumed that both the rate of sedimentation and the constant specific activity of the deposited material are constant. For age-dating by <sup>210</sup>Pb, we used the upper part of the vertical profile, in which the change in <sup>210</sup>Pb activity was the most pronounced. The vertical profile of technogenic <sup>137</sup>Cs was used as an additional confirmation of the dating, assuming that its supply began around 1952.

#### 2.5. Mathematical Processing Radioactivity Measurements

When interpreting the data, the REE concentrations were normalized to the composition of the North American shale (NASC) [39]. To characterize the REE distribution spectrum, the values of the cerium (Ce<sub>an</sub>) and europium (Eu<sub>an</sub>) anomalies as well as the ratio of light REE to heavy REE (LREE/HREE) were calculated according to [40]

$$\text{Ce}_{\text{an}} = (2\text{Ce}_n)/(\text{La}_n + \text{Pr}_n);$$

$$\text{Eu}_{\text{an}} = (2\text{Eu}_n)/(\text{Sm}_n + \text{Gd}_n);$$

$$(\text{LREE}/\text{HREE})_{\text{NASC}} = (\text{La}_n + 2\text{Pr}_n + \text{Nd}_n)/(\text{Er}_n + \text{Tm}_n + \text{Yb}_n + \text{Lu}_n),$$

where  $X_n$  is normalized to NASC composition values.

The REE pattern was also described with the ratios (La/Yb)<sub>n</sub> and (La/Sm)<sub>n</sub> normalized to NASC.

To assess the sources of matter input, the enrichment factors (EF) were calculated relative to the average composition of the upper continental crust (UCC) [41]:

$$EF = (TE/Al_{\text{sample}})/(TE/Al_{\text{UCC}}),$$

where TE/Al is the ratio of the element to aluminum in the sample and in UCC, respectively. Low EF values (less than 3) suggest predominantly detrital sources of the element.

Statistical data processing included the calculation of correlation coefficients and, based on the correlation matrix, a hierarchical analysis with clustering of variables using the Statistica 7 program. Clustering of variables was carried out using the Ward's method, and Pearson's correlation coefficient was used as a linkage distant.

### 3. Results

#### 3.1. Lake Inkino of the Floodplain

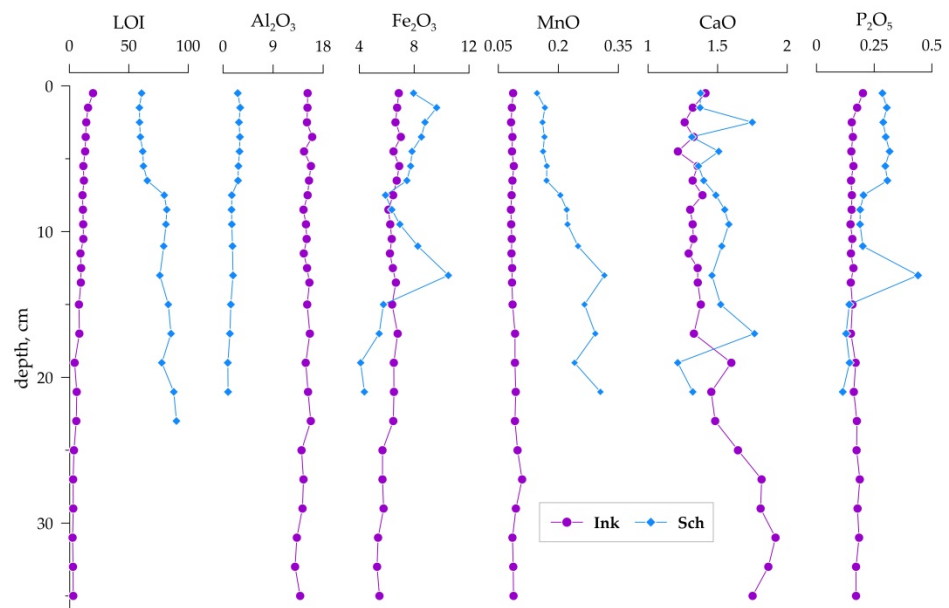
The LOI values decrease gradually down the core from 19.9 to 3.2% (Table 1). The content of Al<sub>2</sub>O<sub>3</sub> varies from 13.0 to 16.0%, its distribution over the column is uneven, and there is a gradual decrease in Al towards the lower parts of the column (Figure 2). A similar vertical distribution is typical for Mg, K, Fe, as well as for a number of trace elements (Li, Be, Sc, V, Ni, Rb, Cs, etc.). The distribution of Ca and Sr shows higher contents in the lower part of the core (at horizons deeper than 18 cm). Distribution of many trace elements as well as LOI shows a distinct boundary of 18 cm, below which the contents of elements (except for Ca and Sr) decrease. Manganese has a maximum content at 26–28 cm horizon, while its content decreases in deeper horizons. Vertical distribution of Cd, P, Pb, Bi, and Zn shows high contents of elements in the top 2 cm of the core and a gradual decrease towards the bottom of the core (Figure 3). Despite the revealed distribution trends, the elemental composition of Lake Inkino sediments is very uniform. The value of the relative standard deviation (RSD), which characterizes the scatter in the abundances of elements, varies from 3 to 41%. At the same time, for many elements, the RSD values do not exceed 15%, and the largest scatter was obtained for chalcophile elements: Cu (18%), As (21%), Mo (41%), Cd (37%), and Bi (17%).

**Table 1.** Major and trace elements concentration in lake sediments, river suspended particulate matter (SPM)m and upper continental crust (UCC).

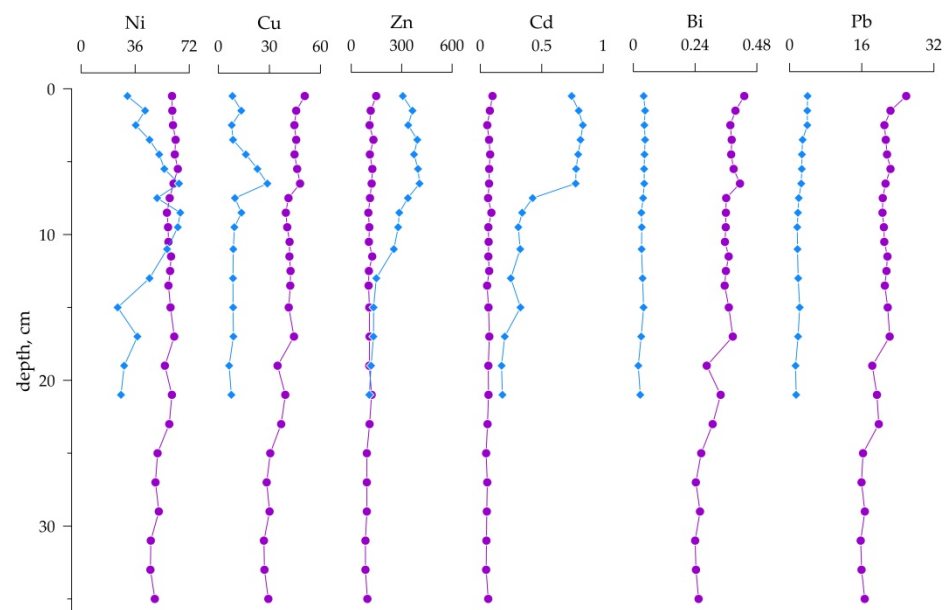
Element	Unit	Lake Inkino		Lake Shchuchie		Organic–Mineral Lake Sediments	Mineralized Lake Sediments	Permafrost-Free Zone River SPM	WSL River SPM	UCC
		Range	0–1 cm	Range	0–1 cm	[11,25]	[35]	[41]		
Na		0.82–1.47	0.82	0.02–0.09	0.05	0.4	1.2	0.37	0.37	0.42
Mg		1.26–1.59	1.26	0.07–0.15	0.07	0.5	1.1	0.55	0.44	3.48
Al		6.85–8.48	6.85	0.45–1.64	0.45	2.2	6.9	3.09	2.59	1.92
P		0.06–0.09	0.06	0.03–0.19	0.03			0.70	0.49	0.05
K	%	1.65–2	1.65	0.05–0.13	0.05	0.6	2.2	0.70	0.65	2.76
Ca		0.87–1.37	0.87	0.87–1.26	0.87	1.3	1.4	1.71	0.89	0.09
Ti		0.38–0.48	0.38	0.01–0.03	0.01			0.78	0.81	0.07
Mn		0.06–0.08	0.06	0.11–0.24	0.11	339	225	1.42	0.80	0.56
Fe		3.7–4.91	3.70	2.86–7.34	2.86	1	3.1	7.56	6.98	3.52
LOI		2.7–19.9	19.9	58.9–90.1	60.7	50%–70%	15%–30%			

Table 1. Cont.

Element	Unit	Lake Inkino		Lake Shchuchie		Organic–Mineral Lake Sediments	Mineralized Lake Sediments	Permafrost-Free Zone River SPM	WSL River SPM	UCC
		Range	0–1 cm	Range	0–1 cm					
Li		31.2–46.1	43.62	1.27–2.46	1.82	10	26	15.6	11.6	24
Be		2–2.6	2.35	0.33–0.71	0.53					2.1
Sc		14.3–18.9	16.9	1–2.31	1.58					14
V		106–142.7	136	7.2–24.2	20.7	32	75	61.4	57.9	97
Cr		76.6–110.1	97	7.4–30.3	21.4	44	57	42.7	41.5	92
Co		15.3–23.2	22.7	5.5–141	47	7	9	32.7	24.6	17.3
Ni	µg/g	46.2–64.4	61	7.69–66	31	23	33	26.9	24.1	47
Cu		26.8–50.8	51	4.37–28.8	8.3	20	27	16.4	14.6	28
Zn		84–149	149	25.7–406	307	110	71	112.8	90.1	67
Ga		14.7–20	17.8	0.86–1.51	1.27			8.46	6.65	17.5
As		3.8–9.5	7.43	7.2–13.3	9.29			34.8	19.3	4.8
Rb		79.3–117.2	110	3.97–7.04	5.14			36.3	28.8	84
Sr		122–174	126	38.8–59.1	49.9	171	108	180	132	320
Y		22.4–27.4	24.1	2.07–7.09	5.39			9.75	9.01	21
Zr		92–115	99	6.04–14.7	9.88			34.8	34.6	193
Nb		9.2–10.7	9.17	0.43–1.06	0.82			15.7	15.1	12
Mo		0.3–1.6	1.44	1.21–2.52	1.37			0.49	0.46	1.1
Cd		0.1–0.5	0.55	0.08–0.83	0.74	0.43	0.2	0.35	0.32	0.09
Sb		1.1–1.5	1.5	0.15–0.38	0.28	0.85	0.39	0.73	0.72	0.4
Cs		4.5–7	6.55	0.31–0.44	0.32			2.4	1.65	4.9
Ba		428–500	471	165–257	165	163	231	617	404	628
La		27.7–31.1	27.7	1.6–5.4	4.36	6.80	23.20	13.9	12.6	31
Ce		59.6–66.7	60.3	3.78–13.9	12.1	14.80	45.20	28.9	26.4	63
Pr		6.7–7.5	6.72	0.43–1.59	1.26			3.2	2.96	7.1
Nd		26.8–29.7	26.8	1.85–6.64	5.35	5.40	19.60	12.4	11.6	27
Sm		5.5–6.4	5.75	0.43–1.51	1.16	1.10	4.30	2.53	2.31	4.7
Eu		1.2–1.4	1.23	0.09–0.34	0.26	0.30	0.90	0.59	0.54	1
Gd	µg/g	4.9–5.5	4.93	0.4–1.38	1.1	1.20	4.40	2.5	2.28	4
Tb		0.7–0.9	0.75	0.06–0.21	0.17	0.20	0.70	0.34	0.31	0.7
Dy		4.1–4.7	4.32	0.34–1.22	0.95			1.92	1.78	3.9
Ho		0.8–0.9	0.83	0.07–0.24	0.19			9.75	0.33	0.83
Er		2.3–2.8	2.47	0.22–0.73	0.55			0.36	0.99	2.3
Tm		0.3–0.4	0.34	0.03–0.1	0.08			1.06	0.14	0.3
Yb		2.1–2.8	2.48	0.21–0.71	0.57	0.50	2.20	0.15	0.93	1.96
Lu		0.3–0.4	0.35	0.03–0.1	0.07	0.10	0.30	0.97	0.14	0.31
Hf		2.5–2.9	2.48	0.15–0.43	0.29	1.10	5.40	0.14	4.63	5.3
Ta		0.7–0.8	0.67	0.03–0.06	0.04			4.8	1.07	
W		1.4–1.8	1.72	0.1–0.18	0.18			1.17	1.02	1.9
Tl		0.3–0.5	0.45	0.02–0.35	0.21			0.95	0.17	0.9
Pb		15.8–25.9	25.85	1.12–3.97	3.97	14	14	0.2	12.8	17
Bi		0.2–0.4	0.43	0.02–0.05	0.04			12.8		0.16
Th		8.6–10.9	9.79	0.6–2.05	1.4				3.02	10.5
U		1.8–2.7	2.48	0.15–0.31	0.18			3.78	0.72	2.7



**Figure 2.** Vertical distribution of LOI and element oxides (in %m/m) in Ink and Sch sediments.



**Figure 3.** Vertical distribution of trace elements (in ppm) in Ink and Sch sediments.

### 3.2. Lake Shchuchie of the 2nd Terrace

The LOI value varies from 59 to 90%, which corresponds to sapropels (Table 1). The LOI gradually increases with depth. According to its chemical composition, the core can be divided into two heterogeneous sections: 0–7 cm and 7–24 cm. In the upper part, there is a higher aluminum content and lower LOI values. The vertical distribution of Al, Mg, K, Ti, Sc, Rb, Cr, Zn, Cs, Cd, Bi, etc., shows distinct division into two intervals—a higher and more uniform content at the depth 0–7 cm and lower and decreasing with depth in the interval of 7–24 cm (Figures 2 and 3). The contents of Pb are distributed in a similar way; however, in the depth 0–3 cm, its content is 1.5–2 times higher than in the underlying layers. Fe, P, Y, and REEs are characterized by higher uniform contents in the interval of 0–7 cm and decrease deeper; however, in the interval of 12–18 cm, the contents show a maximum. Mn, Mo, and Ba show lower contents in the interval of 0–7 cm, and deeper, their contents increase and have peaks. Sediments of the Lake Shchuchie are more heterogeneous in composition compared to those of Lake Inkino. The RSD value varies from 9 to 57%. Co,

Cu, Zn, Cd, Tl, Pb, and P show the greatest variability (the RSD value of these elements is 40% and higher).

### 3.3. Rare Earth Elements

Distribution of REEs in sediments of Lake Inkino indicates a high homogeneity. The shale-normalized REE spectrum varies very little, being quite close to that of the shale [39], but there is a slight enrichment of medium masses and depletion of heavy masses REEs relative to shale (Figure 4a). Lake Shchuchie’s sediments are depleted in REEs relative to shale [39] (Figure 4b). The spectrum shows enrichment of medium masses REEs, as in the Ink sediments. There is a small but detectable positive cerium anomaly in the Sch sediments ( $Ce_{an}$  values vary from 0.99 to 1.13).

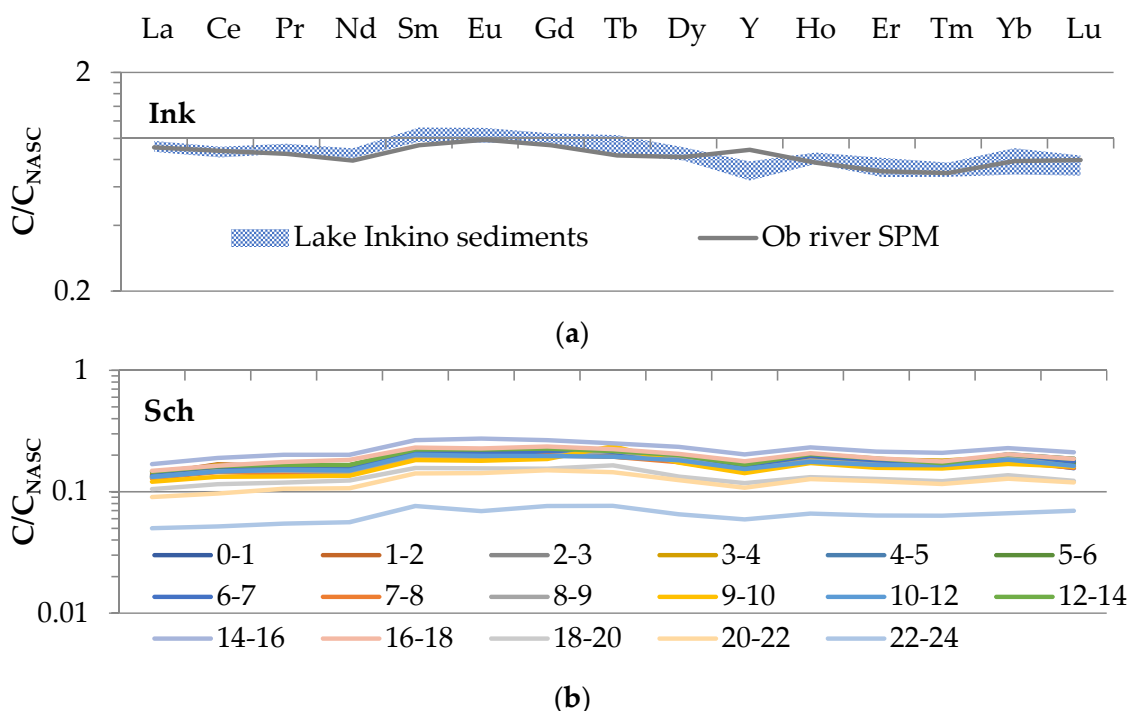


**Figure 4.** (a) Range of REE-normalized values in Lake Inkino sediments and in Ob River SPM [42]; (b) REE-normalized values in Shchuchie Lake sediments. The numbers indicate the different depth horizon, shown by lines of different colors.

### 3.4. Cluster Analysis

Hierarchical cluster analysis allows to group the elements in accordance with the similarity of their distribution (Figure 5).

There are three clusters of elements in Lake Inkino sediments:

- Ink1—Na, Ca, Sr, Mn, and P; Ti—the group combines elements showing content increases in horizon of 18–36 cm. All these elements have negative correlation with Al;
- Ink2—Mg, Al, K, Ba, W, Cr; Fe, Ni, Li, V, Cs, Be, Tl, Sc, Ba, Rb, Th, Mo, and U; Co, Cu, Bi, Pb, and As; Sb, Zn, Cd, and Ag;
- Ink3—REEs, Y, and Zr.

Clusters Ink2 and Ink3 are negatively correlated with cluster Ink1.

There are three clusters of elements in Lake Shchuchie sediments, too:

- Sch1—Na, Ca, and Sr; REEs, Y, Cs, and U;
- Sch2—Mg, Ti, Rb, Zr, Th, Cr, Zn, K, V, Bi, Cu, P, and Fe; Al, Cd, Pb, and Sb; Co, Ni, As, and Cu;
- Sch3—Mn, Mo, and Ba.



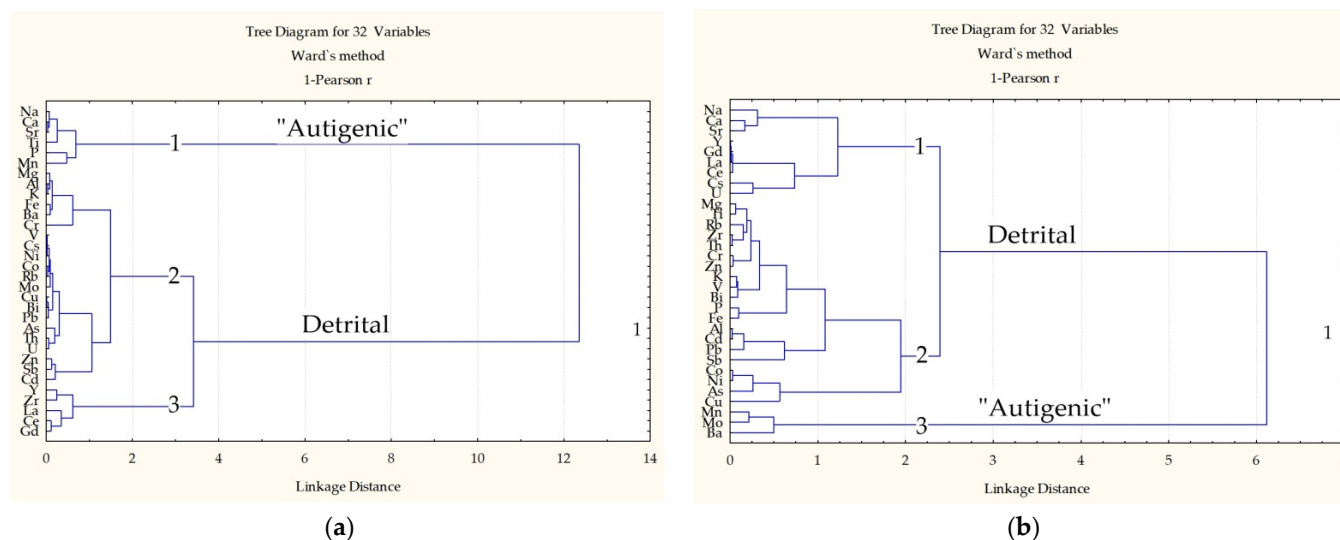


**Figure 5.** Tree diagram for Lakes Inkino (a) and Shchuchie (b) sediments elemental composition.

### 3.5. Enrichment Factors

Ink sediments are similar in composition to the average composition of the upper continental crust (UCC) [41], and enrichment is not detected for most elements. The variance of EF values in the sediments core is quite low, which suggests a homogeneity of the sediments composition and its coherence to the detrital matter. Only two elements show EF values exceeding 3: Cd and Sb, indicating the additional source of their input (Figure 6). Vertical variability of EF values was revealed for Mo, Co, Pb, Cu, Zn, Bi, and Cd. These elements show decreasing enrichment with depth. Sch sediments are enriched with many elements compared to UCC. EF values greater than 3 were calculated for Ba, Cu, Ca, Sb, Ni, Fe, P, Mo, As, Mn, Zn, Co, and Cd (Figure 6). There is an increase in EF with depth for many elements with high EF values. The EF for Mn sharply increases at a depth of 7 cm; the EF for Mo and Ba increase simultaneously with Mn EF.

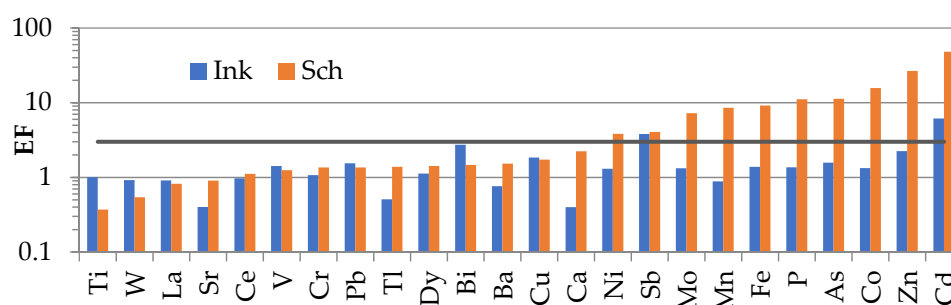


**Figure 6.** Enrichment factors of elements in upper horizons of Ink and Sch sediments.

### 3.6. Radioactivity of Lake Sediments

The estimate of the sedimentation rate in Inkino is 0.75 mm/year, which coincides with both the upper layers for  $^{210}\text{Pb}$  and for  $^{137}\text{Cs}$ . Thus, the upper 11 cm of core Ink has accumulated over the past 150 years. It appears to be impossible to estimate the sedimentation rate in Sch sediments by  $^{210}\text{Pb}$  due to low activity and failed measurement statistics. The estimate for  $^{137}\text{Cs}$  is about 2.3 mm per year. Based on this estimate, the upper 24 cm core has accumulated over the past 100 years.

## 4. Discussion

Sediments of the two lakes are sizably different in the organic matter content: Ink sediments refer to the clastic type of sediments, while Sch sediments refer to sapropels [43]. It was previously reported that sapropels are widespread in the south of western Siberia [11,25].

As a result, the contents of most trace elements are controlled by organic matter, which either promotes additional accumulation of heavy metals or leads to a dilution of the detrital matter in the sediments [44,45].

#### 4.1. Lake Inkino

Vertical distribution of LOI values in Ink sediments indicates the accumulation of organic matter and chemically bound water in minerals in the upper parts of the core. The upper layer of Ink sediments shows higher concentrations of a number of elements (P, Cu, Zn, Cd). Some of these elements are biogenic and participate in the processes of photosynthesis, nitrogen metabolism, etc. [44]. An increase in the concentrations of these elements in the upper parts of the sediment is considered to be associated with their input together with organic matter, whereas a decrease in their concentration in the lower parts of the core can be linked to processes of organic matter decomposition, which liberates these elements to the porewater [13,46].

A comparison of the composition of Ink sediments with that of suspended particulate matter (SPM) of the Ob River shows the similarity of their elemental composition (Figure 7). The difference between the contents of such elements as Al, Ti, V, Cr, Co, Ni, and Ba in the Ob SPM and in the upper sediment layer of the lake does not exceed 13%. However, the Ob River SPM shows significantly higher content of Fe, Mn, as well as Cu, Zn, As, Pb, and Ca compared to the lake sediments. This enrichment of the Ob SPM was reported by different authors both for the average river SPM composition [42] and for the Ob SPM near the mouth of its tributary, the Irtysh River [47]. The content of Mn is three times higher in the Ob River SPM compared to the Lake Inkino sediments. Compared to the world river SPM average, the WSL rivers exhibited lower concentrations of all elements except Mn and P, which relates to high content of organic detritus in river SPM. This reflects presence of peat particles and vegetation debris as important components of RSM. Further, WSL rivers contain sizable amounts of  $Mn^{2+}$  oxidation products, which are supplied from surrounding lakes and bogs, leading to an enrichment in Mn [35]. According to ref. [48], SPM of the rivers of the Asian part of Russia is also enriched in Mn, Fe, Cr, Ni, Cu, and Zn as well as in Ca and Sr. In terms of aluminum content, Ink sediments and river SPM are close to the UCC average composition [41]; the contents of Ni, Rb, Ba, and U are also similar.

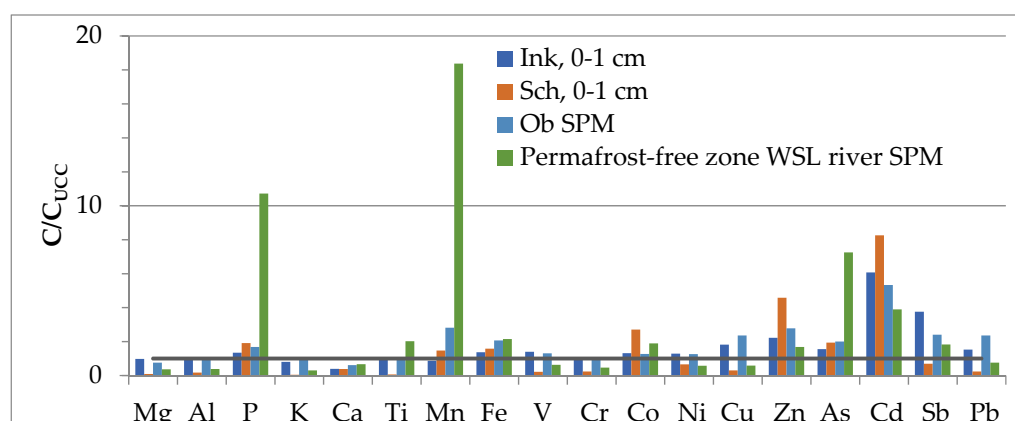


**Figure 7.** UCC-normalized element concentrations in lake sediments and SPM of Ob river [49] and of the permafrost-free zone rivers of WSL [35].

The REE composition and pattern of the Ink sediments are similar to those of the Ob SPM [49] in terms of total REEs,  $Ce_{an}$  and  $Eu_{an}$  values, and ratio of light and heavy REEs (Figure 4a, Table 2). Thus, the main source of the sedimentary material in the Lake Inkino is the Ob River SPM, which is consistent with the location of this lake in the floodplain of the river. The lower contents of Fe and Mn compared to the Ob SPM may be due to the reduction and mobilization of these elements during sedimentation in the presence of organic matter [50].

**Table 2.** REEs distribution features in the upper layer of Sch and Ink sediments and in other objects of western Siberian lowland (WSL).

Object	$\Sigma$ REE	Ce <sub>an</sub>	Eu <sub>an</sub>	(La/Yb) <sub>n</sub>	(La/Sm) <sub>n</sub>	(LREE/HREE) <sup>NASC</sup>	References
Ink, 0–1 cm	145.0	0.96	1.02	1.09	0.86	1.15	This study
Sch, 0–1 cm	28.2	1.12	1.02	0.73	0.67	0.93	
Different lake BS types in western Siberian lakes							
Organogenic sediments	31.5		1.14	1.32	1.10		[11]
Clastic sediments	106.3		0.91	1.02	0.96		[11]
River SPM of WSL							
Ob River	148.6	1.00	1.06	1.16	0.98	1.15	[49]
Small rivers of the permafrost-free zone	69.0	0.94	1.03	1.39	0.98	1.32	[35]
Average WSL	63.3	0.94	1.03	1.31	0.97	1.27	[35]

Based on Ca and Al vertical distribution, which shows an increase in the content of Ca with a simultaneous decrease in the content of Al in layers deeper than 18 cm (Figure 2), it can be assumed that carbonate minerals occur in the interval of 18–36 cm, which is possibly associated with authigenic Ca, Mg, or Fe carbonate formation. At the same time, in contrast to carbonate-type sediments described in ref. [11], there is no significant enrichment in calcium, magnesium, and strontium—elements associated with authigenic carbonates—in the entire core. The accumulation of authigenic carbonates is widespread in lake sediments in the more southern regions of western Siberia [51–53]. The age of the boundary layer of 18 cm is estimated at approximately 240 years. In addition to the difference in the accumulation of Al and Ca, the intervals above and below this depth also differ in the REEs composition. Above this layer, there is no Ce anomaly (the Ce<sub>an</sub> value is 0.96–0.98), and below, there is a weakly expressed negative Ce anomaly (Ce<sub>an</sub> 0.91–0.93). The Ce<sub>an</sub> values are negatively correlated with the Mn content (correlation coefficient –0.65), which suggests that accumulation of REEs is not related to the formation of oxides and hydroxides of Mn. In addition, in the interval of 18–36 cm, there is an enrichment in light REE. (La/Yb)<sub>n</sub> ratio in the interval of 18–36 cm is 1.21–1.35, whereas in the surface layers, it is 1.05–1.13. There is a direct correlation between calcium and light REEs (the correlation coefficient between (La/Yb)<sub>n</sub> and Ca is 0.89). The change in the mobility of light REEs relative to heavy REEs may be associated with a change in the pH [40,54].

The combination of elements during hierarchical correlation analysis into one cluster, as a rule, reflects their accumulation of elements in certain carrier minerals or mineral associations. The Ink2 cluster, which combines a large group of elements, including Al, Mg, and K, is associated with the aluminosilicate phase of sediment (clay and clastic fraction). In contrast, the cluster Ink3 (REEs, Y, Zr) could be associated with zircons, which form a heavy clastic fraction in the sediment. Placer zircon deposits are known in Tomsk region [55]. The vertical distribution of elements from the Ink3 cluster shows higher contents in the interval 0–18 cm, which indicates an accumulation of heavy clastic fraction in the upper part of the core, which is possibly associated with a more intense input of clastic material from the lake catchment as a result of an increase in atmospheric precipitation during this period.

Clusters Ink2 and Ink3 reflect a detrital source of matter, which is opposed to an authigenic (chemogenic) source—cluster Ink1, which combines elements increasing in the range of 18–36 cm: Ca, Na, Sr, P, Ti, P, and Mn. Titanium in sediments shows little mobility in contrast to manganese and phosphorous [56]. It is difficult to assume co-precipitation of these elements in one mineral phase during low-temperature diagenetic processes. Thus, the positive correlation between Mn and Ti (correlation coefficient 0.74) may be due to the coincidence of several factors, such as an increase in sediment grain size (which may lead to an increase in titanium content [56]) and increased oxidation processes in the watershed or in sediments, which may lead to Mn accumulation. Calcium exhibits a direct correlation

with Al in the interval 0–18 cm; thus, Ca is suggested to be predominantly part of clastic minerals, and carbonate accumulation does not occur in this interval, and a negative correlation is in the interval 18–36 cm, which confirms the assumption of chemogenic carbonate accumulation in this interval although not on a large scale given that calcium concentrations are rather low—1.04%–1.37%. Thus, Ink sediments are clearly subdivided into two intervals, which is apparently determined by a change in the climatic conditions during sedimentation: drier and warmer conditions, which are favorable for carbonate sedimentation and for the 18–36 cm interval, and wetter and cooler, which are favorable for an increase in the input of heavy clastic fraction—for the upper interval. Further studies are needed to assess whether this is linked to the change of the river bed position, degree of lake overgrowth by macrophytes, amount of PSM delivered from the Ob River during the spring flood, or simply due to the change of human activity in the vicinity of the lake.

#### 4.2. Lake Shchuchie

According to the composition of sediments, the Sch core is clearly divided into two horizons: the upper 7 cm of the core is characterized by a higher proportion of detrital matter and an increase in the proportion of organic matter with depth between 7 and 24 cm. Based on the assessment of sedimentation rates, the 7 cm boundary has an age of about 30 years. The upper 7 cm is very homogeneous in composition, and the uppermost layers are not distinguished by the concentration of biogenic elements, as it was revealed in Ink sediments. An increase in the proportion of detrital matter may indicate an increasing intensity of mineral soil erosion at the watershed.

Sch sediments are depleted in most elements compared to the composition of the Ob River SPM. The concentrations of Na, Mg, Al, K, Ti, Sc, V, Cu, Ga, Rb, Zr, Y, light REEs, Nb, Cs, Ta, W, Pb, Bi, and Th in Sch sediments are 5–20 times lower than in the Ob SPM, which reflects dilution of the detrital matter of sediment with organic matter. Sch sediments are also depleted in Ca, Mn, Fe, Ni, As, Sr, and Ba compared to the Ob SPM; their concentrations in river SPM are 1–3 times higher. The concentrations of P, Co, Zn, Mo, and Cd are 1.5–2.5 times higher in Sch sediments (Figure 7).

Based on the EF values, additional sources other than the detrital ones can be suggested for the following elements: Co, Ni, Cu, Zn, As, Mo, Cd, Sb, Ba, P, S, Ca, Mn, and Fe. The relative enrichment of the upper horizon compared to the lower ones was obtained for Ni, P, Zn, Co, and Cd, which may indicate both the accumulation of biophilic elements (nutrients such as Zn and P) associated with organic matter and recent increase in the input of these elements, in particular from anthropogenic sources [1–3,5,8,9,20]. The enrichment in other elements increases with depth, which may be linked to diagenetic processes (precipitation of manganese and iron oxides, authigenic mineral formation, etc.) [50]. The EF values for manganese sharply increase at a depth of 7 cm, and the contents of Mo and Ba increase synchronously with Mn. The EF values for manganese sharply increase at a depth of 7 cm, and the contents of Mo and Ba increase synchronously with Mn. This is likely to occur due to the fact that the content of organic matter, which is enriched in Mn, Mo, and Ba, also sharply increases at this depth [44]. The additional accumulation of manganese occurs in the range of 12–24 cm. It is interesting to note that simultaneous precipitation of oxygenized Ce does not occur since the value of  $Ce_{an}$  is inversely correlated with Mn (Figure 8). Low  $Ce_{an}$  values (0.99–1.08) were obtained in the 7–24 cm interval where manganese accumulates, while in the 0–7 cm interval, the  $Ce_{an}$  value is 1.12–1.13. Thus, the  $Ce_{an}$  value is a feature of the sedimentary material entering the lake rather than a result of the coprecipitation of Mn and Ce in oxygenized conditions.

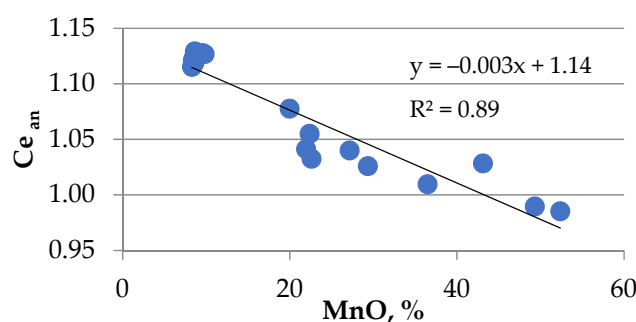


**Figure 8.** MnO vs. Ce<sub>an</sub> scatter plot.

According to the REE distribution, Sch sediments are characterized by a 5-fold depletion compared to the Ob SPM (Table 3), which may refer to dilution by organic matter [11]. Sch sediments differs from the Ob SPM not only in REE content but also in the presence of positive Ce<sub>an</sub> in the upper 7 cm of the core and depletion of light REE throughout the depth. According to Strakhovenko et al. (2010) [11], organogenic lake sediments in the south of western Siberia are characterized by enrichment in light REEs. Light REEs are more mobile during chemical weathering, and their mobility increases with decreasing pH [54]. Because Lake Shchuchie shores are waterlogged, perhaps this behavior of REEs is caused by the acidic environment [28] in the lake due to the influx of humic acids from the surrounding mires.

**Table 3.** Contamination factor values in sediments of Lakes Inkino and Shchuchie.

C <sub>f</sub>	V	Cr	Co	Ni	Cu	Zn
Sch	2.9	2.9	8.5	4.0	1.9	11.9
Ink	1.0	1.2	1.1	1.0	1.2	1.4
C <sub>f</sub>	Cd	Sb	W	Tl	Pb	Bi
Sch	9.5	1.1	1.8	10.0	3.5	2.2
Ink	2.6	1.2	1.0	0.9	1.2	1.2

Clusters of elements identified during the correlation analysis characterize mineral associations in sediments of Lake Shchuchie. Detrital and authigenic complexes of elements are revealed similar to Ink BS. Cluster Sch1 is associated with accumulation of detrital minerals (as we can tell from the set of chemical elements [57]): plagioclases (Na, Ca, Sr) and monazite (REEs + Y, Cs, U)—a weathering-resistant mineral of the heavy fraction. This is consistent with numerous occurrences of monazite ores reported on the territory of the Tomsk region [58]. We assume that the elements related to monazite (REEs, U, Cs) are unevenly distributed over the depth of the core: their concentrations are uniform in the interval of 0–7 cm, have a pronounced peak at a depth of 14–16 cm, and sharply decrease at deeper horizons. Most elements exhibit significant positive correlations with Al, which suggests that these elements are related to the aluminosilicate mineral phase (clusters Ink2 and Sch 2) (Figure 9). The Sch3 cluster is interpreted as being controlled by the authigenic manganese oxides.

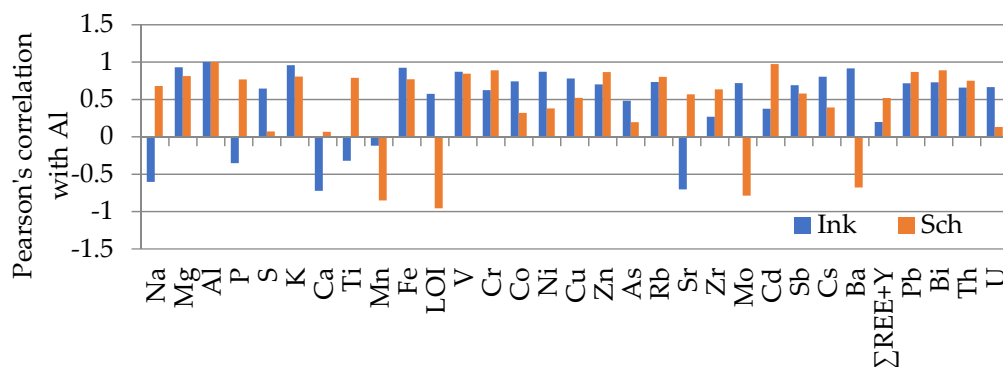


Figure 9. Correlation coefficients between the content of aluminum and other elements and LOI.

4.3. Assessment of Anthropogenic Impact

Since organic matter affects the content of heavy metals, it is reasonable to compare sapropel and clastic lake sediments separately. Compared to lakes in the south of western Siberia [25], lake sediments in the middle course of the Ob River are enriched in Co, Ni, Zn, and Cd; Ink sediments show higher contents of Cr, Cu, and Sb (Figure 10). Note that there is no sign of local Pb pollution in lake sediments due to the rather pristine context of the middle course of the Ob River sampled in this work, unlike in the case of the lake sediments of industrialized regions [12]. Therefore, elevated concentration of heavy metals can be associated with both the features of the lake’s watershed and global anthropogenic pollution.

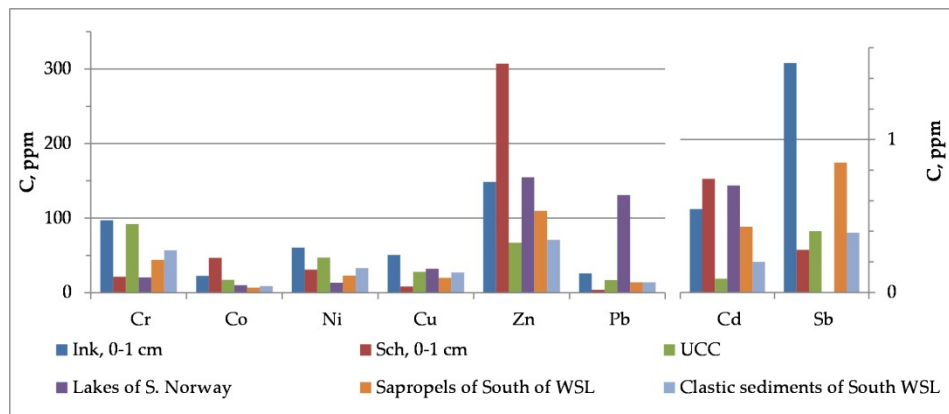


Figure 10. Heavy metal content in the studied lake sediments, in UCC [41], in the lake sediments of different types of western Siberia [25] and of south Norway [12].

To describe the contamination by toxic elements of the lake sediments, we defined a contamination factor ( $Cf_i$ ) accordingly:

$$Cf_i = C^{0-1}_i / C^n_i$$

where  $C^{0-1}_i$ —the concentration of the element  $i$  in upper 0–1 cm layer of sediments, and  $C^n_i$ —the concentration of the element in preindustrial time [59]. Preindustrial level in the western Siberia corresponds to the end of XIX century, corresponding to the depth of 24 cm in Shchuchie sediments and 8 cm in Inkino sediments.

$Cf$  values greater than 1 suggest moderate sediment contamination with Cr, Co, Cu, Zn, Cd, Sb, Pb, and Bi (Table 3). Sch sediments show higher  $Cf$  values, which is caused not so much by anthropogenic pollution as by bioaccumulation of heavy metals.  $Cf$  values in the Ink sediments corresponds to a moderate level of pollution.

## 5. Conclusions

Sediments of the studied lakes are related to two main types—clastic (Lake Inkino), located in the floodplain of the Ob River, and organogenic (Lake Shchuchie), located at the river terrace in the vicinity of peat bogs. The difference in the landscape position of the two lakes determines the patterns of heavy metals accumulation in sediments. The two lakes are likely to have different composition of accessory minerals of heavy fraction (rare-metal minerals) despite the proximity of sampling sites. The patterns of the REEs suggest the similarity of the Lake Inkino sediments to the Ob River suspended particulate matter. Sediments of the Lake Shchuchie are depleted in REE due to the high content of organic matter but enriched in Mo, Mn, P, Fe, As, Zn, and Cd. Diagenetic processes proceed differently in sediments of two studied lakes. The sampled cores allow reconstructing the history of sedimentation over the past 100 years or more. Sediments of both lakes are enriched in Cd, Sb, and other trace metals. The enrichment in these metals is mainly governed by natural processes; however, compared to preindustrial sediments, there is an enhanced recent input of Cr, Co, Cu, Zn, Cd, Sb, Pb, and Bi in the upper part of the sediment core.

**Author Contributions:** Conceptualization, V.P.S., O.S.P. and S.N.V.; methodology, V.P.S. and D.P.S.; data curation, L.P.B. and L.G.K.; visualization, A.G.L.; investigation, R.A.A., A.I.O. and V.V.T.; writing—original draft preparation, V.P.S., D.P.S. and S.N.V.; writing—review and editing, V.P.S., D.P.S. and O.S.P. All authors have read and agreed to the published version of the manuscript.

**Funding:** Work has been supported by Russian Fund for Basic Research (grant 19-05-50096). Interpretation of results was carried out partly in accordance with the State Assignment of Ministry of Science and High Education, Russia, Programs No. FMWE-2021-0016. Partial support was provided from grant “Kolmogorov” of MES (Agreement No 075-15-2022-241) and the TSU Program Priority-2030. The study was carried out by using the equipment of the Unique Research Installation “System of experimental bases located along the latitudinal gradient” TSU with financial support from the Ministry of Education and Science of Russia (RF-2296.61321 × 0043, 13.YHY.21.0005, agreement No. 075-15-2021-672).

**Data Availability Statement:** The data presented in this study are partially available on request from the corresponding author.

**Acknowledgments:** The authors are grateful to A.V. Sorochinsky for assistance in the cores sampling and to V.K. Karandashev for performing ICP-MS and ICP-OES.

**Conflicts of Interest:** The authors declare no conflict of interest.

## References

1. Johansson, K.; Andersson, A.; Andersson, T. Regional accumulation pattern of heavy metals in lake sediments and forest soils in Sweden. *Sci. Total Environ.* **1995**, *160–161*, 373–380. [[CrossRef](#)]
2. Smol, J.P. *Pollution of Lakes and Rivers: A Paleoenvironmental Perspective*; Arnold: London, UK, 2002; p. 208.
3. Dauvalter, V.F.; Dauvalter, M.V.; Kashulin, N.A.; Sandimirov, S.S. Chemical composition of bottom sedimentary deposits in lakes in the zone impacted by atmospheric emissions from the Severonikel plant. *Geochem. Int.* **2010**, *48*, 1148–1153. [[CrossRef](#)]
4. Subetto, D.A.; Shevchenko, V.P.; Ludikova, A.V.; Kuznetsov, D.D.; Sapelko, T.V.; Lisitsyn, A.P.; Evzerov, V.Y.; van Beek, P.; Souhaut, M.; Subetto, G.D. Chronology of isolation of the Solovetskii Archipelago lakes and current rates of lake sedimentation. *Dokl. Earth Sci.* **2012**, *446*, 1042–1048. [[CrossRef](#)]
5. Rognerud, S.; Dauvalter, V.A.; Fjeld, E.; Skjelkvåle, B.L.; Christensen, G.; Kashulin, N. Spatial trends of trace-element contamination in recently deposited lake sediment around the Ni–Cu smelter at Nikel, Kola Peninsula, Russian Arctic. *Ambio* **2013**, *42*, 724–736. [[CrossRef](#)] [[PubMed](#)]
6. Leonova, G.A.; Bobrov, V.A.; Krivonogov, S.K.; Bogush, A.A.; Bychinskii, V.A.; Mal'tsev, A.E.; Anoshin, G.N. Biogeochemical specifics of sapropel formation in Cisbaikalian undrained lakes (exemplified by Lake Ochki). *Russ. Geol. Geophys.* **2015**, *56*, 745–761. [[CrossRef](#)]
7. Marx, S.K.; Rashid, S.; Stromsoe, N. Global-scale patterns in anthropogenic Pb contamination reconstructed from natural archives. *Environ. Pollut.* **2016**, *213*, 283–298. [[CrossRef](#)]
8. Slukovskii, Z.I.; Dauvalter, V.A. Features of Pb, Sb, Cd accumulation in sediments of small lakes in the south of the Republic of Karelia. *Trans. Karelian Res. Cent. Russ. Acad. Sci.* **2020**, *4*, 75–94. (In Russian) [[CrossRef](#)]

9. Slukovskii, Z.; Medvedev, M.; Mitsukov, A.; Dauvalter, V.; Grigoriev, V.; Kudryavtzeva, L.; Elizarova, I. Recent sediments of Arctic small lakes (Russia): Geochemistry features and age. *Environ. Earth Sci.* **2021**, *80*, 302. [[CrossRef](#)]
10. Wolfe, A.P.; Miller, G.H.; Olsen, C.A.; Forman, S.L.; Doran, P.T.; Holmgren, S.U. Geochronology of high latitude lake sediments. In *Long-term Environmental Change in Arctic and Antarctic Lakes*; Pienitz, R., Douglas, M.S.V., Smol, J.P., Eds.; Springer: Dordrecht, The Netherlands, 2004; pp. 19–52.
11. Strakhovenko, V.D.; Shcherbov, B.L.; Malikova, I.N.; Vosel, Y.S. The regularities of distribution of radionuclides and rare-earth elements in bottom sediments of Siberian lakes. *Russ. Geol. Geophys.* **2010**, *51*, 1167–1178. [[CrossRef](#)]
12. Rognerud, S.; Hongve, D.; Fjeld, E.; Ottesen, R.T. Trace metal concentrations in lake and overbank sediments in southern Norway. *Environ. Geol.* **2000**, *39*, 723–732. [[CrossRef](#)]
13. Audry, S.; Pokrovsky, O.S.; Shirokova, L.S.; Kirpotin, S.N.; Dupr´e, B. Organic matter mineralization and trace element post-depositional redistribution in Western Siberia thermokarst lake sediments. *Biogeosciences* **2011**, *8*, 3341–3358. [[CrossRef](#)]
14. Flegal, A.R.; Nriagu, J.O.; Niemeyer, S.; Coale, K.H. Isotopic tracers of lead contamination in the Great Lakes. *Nature* **1989**, *339*, 455–457. [[CrossRef](#)]
15. Church, T.M.; Arimoto, R.; Barrie, L.A.; Dulac, F.; Jickells, T.D.; Mart, L.; Sturgess, W.T.; Zoller, W.H. The long-range atmospheric transport of trace elements. A critical evaluation. In *The Long-Range Atmospheric Transport of Natural and Contaminant Substances*; Knap, A.H., Ed.; Kluwer: Dordrecht, The Netherlands, 1990; pp. 37–58.
16. Lisitzin, A.P. Arid sedimentation in the oceans and atmospheric particulate matter. *Russ. Geol. Geophys.* **2011**, *52*, 1100–1133. [[CrossRef](#)]
17. G´elinas, Y.; Lucotte, M.; Schmit, J.-P. History of the atmospheric deposition of major and trace elements in the industrialized St. Lawrence Valley, Quebec, Canada. *Atmos. Environ.* **2000**, *34*, 1797–1810. [[CrossRef](#)]
18. Gashkina, N.A.; Tatsii, Y.G.; Udachin, V.N.; Aminov, P.G. Biogeochemical indication of environmental contamination: A case study of a large copper smelter. *Geochem. Int.* **2015**, *53*, 253–264. [[CrossRef](#)]
19. Michelutti, N.; Simonetti, A.; Briner, J.P.; Funder, S.; Creaser, R.A.; Wolfe, A.P. Temporal trends of pollution Pb and other metals in east-central Baffin Island inferred from lake sediment geochemistry. *Sci. Total Environ.* **2009**, *407*, 5653–5662. [[CrossRef](#)]
20. Bindler, R.; Rydberg, J.; Renberg, I. Establishing natural sediment reference conditions for metals and the legacy of long-range and local pollution on lakes in Europe. *J. Paleolimnol.* **2011**, *45*, 519–531. [[CrossRef](#)]
21. Sarkar, S.; Ahmed, T.; Swami, K.; Judd, C.D.; Bari, A.; Dutkiewicz, V.A.; Husain, L. History of atmospheric deposition of trace elements in lake sediments, ~1880 to 2007. *J. Geophys. Res. Atmos.* **2015**, *120*, 5658–5669. [[CrossRef](#)]
22. Shevchenko, V.P.; Lyubas, A.A.; Starodymova, D.P.; Bolotov, I.N.; Aksenova, O.V.; Aliev, R.A.; Gofarov, M.Y.; Iglovsky, S.A.; Kokryatskaya, N.M. Geochemistry of heavy metals in bottom sediments of small lakes in Pymvashor Trough (Bolshezemelskaya Tundra). *Adv. Curr. Nat. Sci.* **2017**, *1*, 105–110. (In Russian)
23. Tatsii, Y.G.; Moiseenko, T.I.; Razumovskii, L.V.; Borisov, A.P.; Khoroshavin, V.Y.; Baranov, D.Y. Bottom sediments of the West Siberian Arctic lakes as indicators of environmental changes. *Geochem. Int.* **2020**, *58*, 408–422. [[CrossRef](#)]
24. Strakhovenko, V.D.; Ovdina, E.A.; Malov, G.I.; Yermolaeva, N.I.; Zarubina, E.Y.; Taran, O.P.; Boltenkov, V.V. Genesis of organomineral deposits in lakes of the central part of the Baraba Lowland (south of West Siberia). *Russ. Geol. Geophys.* **2019**, *60*, 978–989. [[CrossRef](#)]
25. Strakhovenko, V.; Ovdina, E.; Malov, G.; Yermolaeva, N.; Zarubina, E. Concentration levels and features of the distribution of trace elements in the sapropel deposits of small lakes (south of Western Siberia). *Minerals* **2021**, *11*, 1210. [[CrossRef](#)]
26. Leonova, G.A.; Mal'tsev, A.E.; Melenevskii, V.N.; Miroshnichenko, L.V.; Kondrat'eva, L.M.; Bobrov, V.A. Geochemistry of diagenesis of organogenic sediments: An example of small lakes in southern West Siberia and western Baikal area. *Geochem. Int.* **2018**, *56*, 344–361. [[CrossRef](#)]
27. Maltsev, A.E.; Leonova, G.A.; Bobrov, V.A.; Krivonogov, S.K. *Geochemistry of Holocene Sapropels from Small Lakes of the Southern Western Siberia and Eastern Baikal Regions*; Geo: Novosibirsk, Russia, 2019; p. 444.
28. Vorobyev, S.N.; Pokrovsky, O.S.; Kirpotin, S.N.; Kolesnichenko, L.G.; Shirokova, L.S.; Manasyrov, R.M. Flood zone biogeochemistry of the Ob River middle course. *Appl. Geochem.* **2015**, *63*, 133–145. [[CrossRef](#)]
29. Karandashev, V.K.; Khvostikov, V.A.; Nosenko, S.Y.; Burmii, Z.P. Highly enriched stable isotopes in large scale analysis of rocks, soils, subsoils and bottom sediments using inductively coupled plasma mass spectrometry (ICP-MS). *Ind. Lab. Diagn. Mater.* **2016**, *82*, 6–15. (In Russian)
30. Heiri, O.; Lotter, A.F.; Lemcke, G. Loss on ignition as a method for estimating organic and carbonate content in sediments: Reproducibility and comparability of results. *J. Paleolimnol.* **2001**, *25*, 101–110. [[CrossRef](#)]
31. Dean, W.E., Jr. Determination of carbonate and organic matter in calcareous and sedimentary rocks by loss on ignition: Comparison with other methods. *J. Sedim. Petrol.* **1974**, *44*, 242–248.
32. Bengtsson, L.; Enell, M. Chemical Analysis. In *Handbook of Holocene Paleocology and Paleohydrology*; Berglund, B.E., Ed.; John Wiley & Sons Ltd.: Chichester, Great Britain, UK, 1986; pp. 423–451.
33. Santisteban, J.I.; Mediavilla, R.; L´opez-Pamo, E.; Dabrio, C.J.; Ruiz Zapata, M.B.; Gil Garc´ıa, M.J.; Casta˜no, S.; Mart´ınez-Alfaro, P.E. Loss on ignition: A qualitative or quantitative method for organic matter and carbonate mineral content in sediments? *J. Paleolimnol.* **2004**, *32*, 287–299. [[CrossRef](#)]
34. Bensharada, M.; Telford, R.; Stern, B.; Gaffney, V. Loss on ignition vs. thermogravimetric analysis: A comparative study to determine organic matter and carbonate content in sediments. *J. Paleolimnol.* **2022**, *67*, 191–197. [[CrossRef](#)]



35. Krickov, I.V.; Lim, A.G.; Manasyrov, R.M.; Loiko, S.V.; Vorobyev, S.N.; Shevchenko, V.P.; Dara, O.M.; Gordeev, V.V.; Pokrovsky, O.S. Major and trace elements in suspended matter of western Siberian rivers: First assessment across permafrost zones and landscape parameters of watersheds. *Geochim. Cosmochim. Acta* **2020**, *269*, 429–450. [[CrossRef](#)]
36. Krishnaswamy, S.; Lal, D.; Martin, J.M.; Meybeck, M. Geochronology of lake sediments. *Earth Planet. Sci. Lett.* **1971**, *11*, 407–414. [[CrossRef](#)]
37. Robbins, J.A.; Edgington, D.N. Determination of recent sedimentation rates in Lake Michigan using Pb-210 and Cs-137. *Geochim. Cosmochim. Acta* **1975**, *39*, 285–304. [[CrossRef](#)]
38. Aliev, R.A.; Bobrov, V.A.; Kalmykov, S.N.; Melgunov, M.S.; Vlasova, I.E.; Shevchenko, V.P.; Novigatsky, A.N.; Lisitzin, A.P. Natural and artificial radionuclides as a tool for sedimentation studies in the Arctic region. *J. Radioanal. Nucl. Chem.* **2007**, *274*, 315–321. [[CrossRef](#)]
39. Gromet, L.P.; Dymek, R.F.; Haskin, L.A.; Korotev, R.L. The “North American shale composite”: Its compilation, major and trace element characteristics. *Geochim. Cosmochim. Acta* **1984**, *48*, 2469–2482. [[CrossRef](#)]
40. Dubinin, A.V. *Rare Earth Element Geochemistry in the Ocean*; Nauka: Moscow, Russia, 2006; pp. 1–360. (In Russian)
41. Rudnick, R.L.; Gao, S. *Composition of the continental crust. Treatise on Geochemistry*; Elsevier: Amsterdam, The Netherlands, 2003; Volume 3, pp. 1–64.
42. Savenko, V.S. *Chemical Composition of Suspended Load of the World’s Rivers*; GEOS: Moscow, Russia, 2006; pp. 1–176. (In Russian)
43. Schnurrenberger, D.; Russell, J.; Kelts, K. Classification of lacustrine sediments based on sedimentary components. *J. Paleolimnol.* **2003**, *29*, 141–154. [[CrossRef](#)]
44. Perel’man, A.I. *Geochemistry of Epigenesis*; Springer: New York, NY, USA, 2014; pp. 1–266. [[CrossRef](#)]
45. Baran, A.; Mierzwa-Hersztek, M.; Gondek, K.; Tarnawski, M.; Szara, M.; Gorczyca, O.; Koniarz, T. The influence of the quantity and quality of sediment organic matter on the potential mobility and toxicity of trace elements in bottom sediments. *Environ. Geochem. Health* **2019**, *41*, 2893–2910. [[CrossRef](#)]
46. Petersen, W.; Wallman, K.; Pinglin, L.; Schroeder, F.; Knauth, H.D. Exchange of trace elements at the sediment-water interface during early diagenesis processes. *Mar. Freshw. Res.* **1995**, *46*, 19–26. [[CrossRef](#)]
47. Gordeev, V.V.; Rachold, V.; Vlasova, I.E. Geochemical behavior of major and trace elements in suspended particulate material of the Irtysh river, the main tributary of the Ob river, Siberia. *Appl. Geochem.* **2004**, *19*, 593–610. [[CrossRef](#)]
48. Viers, J.; Dupre, B.; Gaillardet, J. Chemical composition of suspended sediments in World Rivers: New insights from a new database. *Sci. Total Environ.* **2009**, *407*, 853–868. [[CrossRef](#)]
49. Savenko, V.S.; Pokrovsky, O.S.; Dupré, B.; Baturin, G.N. Chemical composition of suspended material in large rivers of Russia and adjacent countries. *Dokl. Earth Sci.* **2004**, *398*, 97–101.
50. Douglas, G.B.; Adeney, J.A. Diagenetic cycling of trace elements in the bottom sediments of the Swan River Estuary, Western Australia. *Appl. Geochem.* **2000**, *15*, 551–566. [[CrossRef](#)]
51. Solotchina, E.P.; Kuzmin, M.I.; Solotchin, P.A.; Maltsev, A.E.; Leonova, G.A.; Danilenko, I.V. Authigenic carbonates from Holocene sediments of Lake Itkul (south of West Siberia) as indicators of climate changes. *Dokl. Earth Sci.* **2019**, *487*, 745–750. [[CrossRef](#)]
52. Zhdanova, A.N.; Solotchina, E.P.; Krivonogov, S.K.; Solotchin, P.A. Mineral composition of the sediments of Lake Malye Chany as an indicator of Holocene climate changes (southern West Siberia). *Russ. Geol. Geophys.* **2019**, *60*, 1163–1174. [[CrossRef](#)]
53. Ovdina, E.; Strakhovenko, V.; Solotchina, E. Autigenic carbonates in the water–biota–bottom sediments’ system of small lakes (south of Western Siberia). *Minerals* **2020**, *10*, 552. [[CrossRef](#)]
54. Lozano, A.; Ayora, C.; Fernandez-Martínez, A. Sorption of rare earth elements on schwertmannite and their mobility in acid mine drainage treatments. *Appl. Geochem.* **2020**, *113*, 104499. [[CrossRef](#)]
55. Nesterenko, G.V.; Kolpakov, V.V.; Boboshko, L.P. Native gold in complex Ti-Zr placers of the southern West Siberian Plain. *Russ. Geol. Geophys.* **2013**, *54*, 1484–1498. [[CrossRef](#)]
56. Calvert, S.E.; Pedersen, T.F. Elemental Proxies for Palaeoclimatic and Palaeoceanographic Variability in Marine Sediments: Interpretation and Application. In *Proxies in Late Cenozoic Paleoceanography*; Hillaire-Marcel, C., De Vernal, A., Eds.; Elsevier: Amsterdam, The Netherlands, 2007; Volume 1, pp. 567–644.
57. Deer, W.A.; Howie, R.A.; Zussman, J. *An Introduction to the Rock-Forming Minerals*, 3rd ed.; The Mineralogical Society: London, UK, 2013; pp. 1–549. [[CrossRef](#)]
58. Rikhvanov, L.P.; Kropanin, S.S.; Babenko, S.A.; Solov’ev, A.I.; Sovetov, V.M.; Usova, T.Y.; Polyakova, M.A. *Zircon-Ilmenite Placer Deposits as a Potential Source for Western Siberian Region Development*; Sars: Kemerovo, Russia, 2001; pp. 1–214. (In Russian)
59. Håkanson, L. An ecological risk index for aquatic pollution control. A sedimentological approach. *Water Res.* **1980**, *14*, 975–1001. [[CrossRef](#)]